Surfaces and Interfaces 41 (2023) 103231

Contents lists available at ScienceDirect

Surfaces and Interfaces

journal homepage: www.sciencedirect.com/journal/surfaces-and-interfaces

Comparing the resilience of macromolecular coatings on medical-grade polyurethane foils

Maria G. Bauer [a,b], Kjetil Baglo [a,c], Luca Reichert [a,c], Jan Torgersen [a,c], Oliver Lieleg [a,b,*]

[a] School of Engineering and Design, Department of Materials Engineering, Technical University of Munich, Boltzmannstraße 15, 85748 Garching, Germany
[b] Center for Protein Assemblies and Munich Institute of Biomedical Engineering, Technical University of Munich, Ernst-Otto-Fischer Str. 8, 85748 Garching, Germany
[c] Institute of Materials Science, Technical University of Munich, Boltzmannstraße 15, 85748 Garching, Germany

ARTICLE INFO

Keywords:
Dopamine coatings
Carbodiimide coatings
Linear tribology
Long-term testing
Sterilization

ABSTRACT

Foils made from elastomeric polymers, such as polycarbonate-based polyurethane (PCU), can combine desirable properties including flexibility, durability, and compliance. Still, their usage is often limited by their strongly autohesive behavior. To overcome this issue, surface coatings can be applied. Here, dopamine-based (dopa) and carbodiimide-mediated (carbo) coatings are compared by assessing their tribological performance and surface properties after long-term sliding tests, and after storage or sterilization. Even though both coating strategies achieve very good lubricity, the dopa-coatings are less resilient than the carbo-coatings. Thus, for such applications where extended sample storage or sterilization is required, covalent coatings should be preferred.

1. Introduction

For medical applications thin, flexible polymeric materials are regularly used [1,2]; they often require anti-adhesive properties, *e.g.,* on the inner sides of intravenous bags or on medical tubings such as catheters. Here, uncontrolled biofouling can (partially) block the device, entail undesired cell ingrowth, lead to infections, and eventually entail device failure [3–5]. For certain applications, the accessible space such an artificial object needs to fit into can be quite limited; thus, the material must be as thin as possible but still sufficiently stable and flexible to fulfill its purpose. For example, when polymeric foils are envisioned as components for cushion-like implants aiming at separating damaged articular surfaces in small joints or replacing intervertebral disks, the polymeric material must endure continuous mechanical loads and deformations and enable a smooth relative movement of the opposing surfaces. Yet, thin spacer materials with appropriate bulk and surface properties are scarce. Thus, coating (thin) polymeric materials to improve their surface properties is the currently preferred method to render them suitable for such medical applications [6–10].

Here, two methods to alter the surface properties of medical-grade carbonate-based polyurethane (PCU) films with initially strongly autohesive properties are compared [11]: first, rather novel dopamine-based (dopa) coatings [12–16], which have gained particular attention as they can readily generate bio-based, intermediate adhesion layers between an extensive range of substrate materials and various top-layer molecules, thus establishing multifaceted properties for bio-medical applications (*e.g.,* anti-biofouling, optimized cell/blood contact surfaces, drug delivery, or bioimaging/-sensing) [17–21]; second, well-established but substrate-/top-layer-wise more restricted, work-intensive carbodiimide-mediated (carbo) coatings [22–25]. Both hydrophilic surface treatments can – when employing a suitable top-layer macromolecule (establishing a hydration layer) combined with a corresponding macromolecular lubricant – enable an efficient gliding motion of two PCU foils by utilizing hydration lubrication and (potentially) sacrificial layer formation [11,26–29]. However, the coatings generated with either method may differ in terms of their stability. Thus, here, the resilience of these coatings towards storage/application conditions, sterilization processes, and prolonged sliding movements is assessed. Additionally, the coatings' ability to prevent wear and abrasion is compared.

2. Experimental section

Unless stated otherwise, all chemicals were obtained from Carl Roth, Karlsruhe, Germany.

* Corresponding author at: Department of Mechanical Engineering and Munich School of Bioengineering, Technical University of Munich, Boltzmannstraße 11, 85748 Garching, Germany.
E-mail address: oliver.lieleg@tum.de (O. Lieleg).

https://doi.org/10.1016/j.surfin.2023.103231
Received 26 May 2023; Received in revised form 24 July 2023; Accepted 30 July 2023
Available online 2 August 2023

2.1. Sample preparation

2.1.1. Polycarbonate-based polyurethane samples

Thermoplastic, aromatic, and medical grade polycarbonate-based polyurethane (PCU, Carbothane™ AC-4085A, Lubrizol Advanced Materials, USA)) was obtained as extruded foils (thickness of ≈ 150–200 μm) from Gerlinger Industries GmbH (Netzschkau, Germany). Those foils had a better surface quality on one side, and all following modifications and examinations were performed on this side only. All further preparation steps required to shape the samples into the desired dimensions were conducted manually: either they were cut with scissors and scalpels or punched into a circular shape with a manual eyelet press (Istabreeze Germany GmbH, Bad Rappenau, Germany).

2.1.2. Cylindrical polydimethylsiloxane (PDMS) samples

Cylindrical polydimethylsiloxane (PDMS) samples (pins) served as a model material to conduct preliminary rotational tribology examinations for assessing coating-lubricant interactions. As previously described by Winkeljann et al. [30], those pins were prepared from the commercially available PDMS system Sylgard 184 (Dow Corning, Midland, MI, USA). A curable solution was prepared by mixing PDMS in a 10:1 ratio with the curing agent and exposing the mixture to vacuum for 1 h (to remove air bubbles). To create pins ($\varnothing = 6.2$ mm), the mixture was filled into a custom-made aluminum mold using a transfer pipette before curing the silicone at 70 °C for 4 h. Since previous studies indicated that there might be unreacted low molecular weight residues left after curing the PDMS [31,32], the samples were further tempered at 110 °C for 2 h.

Prior to any modifications, treatments or tests, all samples (whether made from PDMS or PCU) were cleaned in 80% (v/v) ethanol and deionized water (ddH2O) for 15 min each and then dried.

2.2. Macromolecular lubricants

Here anionic biomacromolecules were examined only (polyanionic macromolecules are typical for biolubricants in the human body) [33]. Further selection criteria: commercial availability in adequate quality/purity; intermediate molecular weight/viscosity. Alginic acid (AlgA, $c = 6\%$, viscosity $\eta_{c=1\%,temp=25°C} = 5 - 40$ mPa $*$ s, Sigma Aldrich, Darmstadt, Germany), γ-poly-glutamic acid (gPGA, $c = 10\%$, MW > 700kDa, Biosynth Ltd., Berkshire, UK), and carboxymethyl-dextran (CM-Dex, $c = 12\%$, $MW = 500$kDa, TdB Labs AB, Uppsala, Sweden) were compared to hyaluronic acid (HA, $c = 8\%$, $MW = 70 - 80$kDa, Biosynth). The respective macromolecule concentrations were adjusted such that a comparable, good tribological performance was achieved. Unless stated differently, the lubricants were prepared in phosphate buffered saline (PBS, $pH = 7.4$, Sigma).

2.3. Surface coatings

To promote interactions with the anionic lubricants, the top-layers in each coating were created from dextran variants which locally provide cationic groups (amines), *i.e.*, Lysine-Dextran and Q-Dextran (TdB Labs). Coatings were applied by employing either a multi-step carbodiimide-mediated coating process [11,21,23,24], or a two-step dopamine-based coating process [12,18,19]. Previously it was shown that those coatings have no undesired effects on the surface roughness, transparency, or flexibility of the employed substrate [11], and this could be confirmed by Fourier-transformed infrared (FTIR, see supplementary information SI 1) and DSC scans (see SI 2).

2.3.1. Carbodiimide-mediated coating process

The coating process for PDMS was conducted as published by Winkeljann et al. [30]. For coating the thermoplastic PCU, the process parameters as described by Bauer, Lieleg [11] were applied. Different process parameters were required to account for differences in the materials' susceptibility to plasma treatment and to compensate for the reduced incubation temperature applicable to PCU (which is due to its relatively low Vicat temperature). In the following process descriptions, different conditions applied to PDMS and PCU, respectively, will be listed in curved brackets as follows: {applied to PDMS/applied to PCU}.

In brief, the surfaces of the samples were activated by employing a low-pressure atmospheric plasma ($p_{abs} = 0.4$ mbar, power supply: {30 W/56 W}, treatment time: {1.5 min/25 min}). Immediately afterwards, each sample was immersed into a silane solution containing 1% (w/v) TMS-EDTA (N-[(3-trimethoxysilyl)propyl] ethylenediamine triacetic acid trisodium salt, abcr GmbH, Karlsruhe, Germany) dissolved in 10 mM acetate buffer at pH 4.5 and incubated at {60 °C/37 °C} for {5 h/8.5 h} to create a silane pre-coating. Subsequently, the samples were dipped into isopropanol to wash off any excess solution. Silane stabilization was conducted at {110 °C & atmospheric pressure/room temperature (RT) & $p_{rel} = -800$ mbar to -600 mbar} for {1 h/16 h}. Afterwards, the samples were washed in 96% (v/v) ethanol to remove any unbound silane molecules. To initiate the macromolecular coupling step, the samples were incubated in a freshly prepared solution containing 5 mM EDC (1-ethyl-3-(3-dimethylaminopropyl)carbodiimide-hydrochloride) and 5 mM sulfo-NHS (N-hydroxysulfosuccimid sodium salt, abcr) dissolved in 100 mM MES (2-(N-morpholino ethanesulfonic acid, AppliChem GmbH, Darmstadt, Germany) buffer at pH 5 for 30 min. Subsequently, the samples were immediately transferred into Dulbecco's phosphate buffered saline (pH = 7.4, DPBS, Sigma-Aldrich Inc., Darmstadt, Germany) containing 0.05% (w/v) lysine-dextran (MW = 150 kDa, TdBlabs, Uppsala, Sweden). After an incubation period of at least 16 h at 7 °C, the macromolecular coupling was finalized, and the samples were cleaned in 80% (w/v) ethanol.

2.3.2. Dopamine-based coating process

As described in [11], both PDMS pins and PCU foils were treated in the same way. To prevent undesired sedimentation and attachment of larger (poly-)dopamine agglomerates onto the surfaces, the samples were positioned vertically in a freshly prepared solution containing 0.4% (w/v) dopamine hydrochloride (Sigma-Aldrich) dissolved in 20 mM HEPES buffer (4-(2-hydroxyethyl)−1-piperazineethanesulfonic acid; pH 8.5) and incubated for 3 h. To wash off excess (poly-)dopamine, the samples were dipped into ddH_2O and subsequently incubated in 20 mM HEPES buffer (pH 7) containing 0.1 (w/v)% Q-dextran (MW = 150 kDa, TdBlabs) at RT overnight. To remove any unbound macromolecules, the samples were dipped into ddH_2O, then into 80% ethanol, and again into ddH_2O. Finally, all samples (independent of how they were coated) were either placed into 20 mM HEPES buffer (pH 7) and stored at 7 °C until further use, or they were dried at RT for at least 24 h (for tests conducted with dry samples).

The successful application of the coatings was assessed by contact angle measurements [11] and FTIR scans (SI 1).

As top-layer molecules, dextrans (MW: 150 kDa) were selected. Such dextrans were previously used in various biomedical studies – especially as a base material for drug delivery applications and tissue engineering purposes [34,35]. Dextrans are commercially available at different molecular weights, and they can carry different functionalizations (*e.g.*, charged residues) [34,36,37]. Based on the findings presented by Imamura et al. [38], a glass transition temperature of > 100 °C was estimated for dextrans with a molecular weight of 150 kDa; this indicates that, at the applied testing temperatures used in this study (max. 30 °C), the dextran layer should not exhibit autohesive behavior. To enable good electrostatic interactions with the anionic macromolecules present in the studied lubricants, Q-dextran was chosen due to its strong cationic character (according to the manufacturer). Moreover, in pretests, we observed a strong interaction of this Q-dextran with dopamine layers, which renders those dextrans suitable components for a dopamine-based coating. However, since such Q-dextran molecules do not possess primary amine groups, applying the carbodiimide-mediated coating

strategy to them was chemically not feasible. Thus, as a suitable alternative, the zwitterionic lysine-dextran was used for carbo-coatings since this molecule comprises the same dextran backbone, was available at the same molecular weight, and, at least locally, carries cationic groups as well.

2.4. Rotational tribology

Friction examinations conducted in static contact between the tribological partners were performed as described in detail in [30]. In brief: a commercial shear rheometer (MCR 302, Anton Paar, Graz, Austria) was equipped with a tribology unit (T-PTD 200, Anton Paar), and a ball-on-cylinder geometry was employed. As a counterpart to the (coated) PDMS cylinders (see above), a steel sphere ($Ø$ = 12.7 mm, Kugel Pompel, Vienna, Austria) was selected. Measurements were performed at a constant normal force of F_N = 6 N such that friction responses in the boundary, mixed, and hydrodynamic regimes could be probed within the accessible speed range, which additionally corresponds to a reasonable velocity range for biomedical applications [39–42]. Based on the Hertzian contact theory [43], an average contact pressure $p_0 \approx 0.31$ MPa was estimated (Young's moduli: E_{steel} = 210 GPa, $E_{PDMS} \approx 2$ MPa; Poisson's ratios: $\nu_{steel} \approx 0.30$, $\nu_{PDMS} \approx 0.49$) [44]. The speed-dependent friction behavior (reported by the coefficient of friction, CoF) was evaluated by running a logarithmic speed ramp decreasing from ≈ 700 to 0.001 mm/s^{-1}. For each measurement, 600 μL of lubricant were required; as all measurements were conducted at 28 °C, a moisture trap was installed around the setup to avoid evaporation of the lubricant.

2.5. Linear tribology: basic measurements

To conduct tribological measurements in migrating contact between the tribological partners, an oscillatory tribology setup employing the same commercial shear rheometer as for rotational tribology measurements was used. However, now it was equipped with a measuring unit (P-PTD200/80/I, Anton Paar) that allows for connecting dedicated sample holders *via* a thread. For all oscillatory tribology experiments conducted here, a sample holder made from stainless steel (which provides a planar surface) was connected to this measuring unit. On the opposing side, a custom-made, maneuverable measuring head (which was based on the measuring head described in detail by Winkeljann et al. [45]) was connected to a measuring shaft for disposable measuring heads (D-CP/PP 7, Anton Paar). The measuring head used here has the same main geometric specifications as the one described in [45]; however, instead of steel spheres, each of the three sample holders was equipped with a custom-made, dedicated PDMS pin (cylinder (Ø 7 mm) having a rounded edge (radius = 3 mm) on the side facing the opposing sample holder); owing to their rounded edges, those dedicated PDMS pins provide a planar surface ($Ø$ = 3 mm), which allows for conducting friction measurements without generating edge artefacts.

For each measurement run, three sets of samples comprising a rectangular sample (~ 12 mm x 8 mm, attached to the stainless-steel bottom plate *via* double-sided adhesive tape) and a circular one ($Ø$ = 6 mm, attached *via* spontaneous adhesion to the PDMS pins mounted in the measuring head) were required. The circular shape of the second sample further reduces the occurrence of undesired edge effects when this circular sample is moved over the rectangular sample during the tribological measurement.

For all linear tribology measurements conducted here, 225 μL of the desired lubricant were applied per set of samples. Since all measurements were conducted at 28 °C, a moisture trap was installed around the setup to avoid evaporation of the lubricant. During the measurements, the circular samples were moved over the rectangular samples at a sliding frequency of 1 Hz and over a sliding angle of 0.15 rad; for such a small ratio of the sliding angle/distance to the radius of the measuring head (18 mm), the movement can be approximated to be almost a straight line. This specific frequency and sliding angle were chosen as they result in maximum sliding velocities of ~ 10 mm/s, which lie in the intermediate range of sliding velocities examined *via* rotational tribology and do not induce inertia-based artefacts at the turning points. Basic measurements were conducted with coated samples in combination with a macromolecular lubricant only. For these measurements, the average contact pressure was (compared to the rotational tribology setup) raised to 0.5 MPa; this was necessary as, in pretests (when employing contact pressures close to the previously employed 0.3 MPa for longer periods) it was observed that the circular foils would tend to lose contact with the PDMS pin mounted in the measuring head. Measurements were run continuously for 45 min and data points were acquired five times per minute.

2.6. Scanning electron microscopy

Uncoated or coated PCU samples were sputtered with gold and examined on a scanning electron microscope (SEM, Jeol JSM-7600F, Jeol (Germany) GmbH, Freising, Germany), employing an acceleration voltage of 10 kV, a working distance of 10 mm, a spot size of 45 and a detector for secondary electrons. Images were acquired such that the interface between the PCU foil and the background was clearly visible. For image evaluation, the software IMS (Imagic, Bildverarbeitung AG, Glattbrugg, Switzerland) was used. The thickness of each coating was estimated by subtracting the mean value obtained for the uncoated samples from the mean value of the coated samples and conducting error propagations.

2.7. Linear tribology: long-term measurements

These long-term tests were run with coated as well as with uncoated samples; in all cases, a 12% CM-Dex solution was used as a lubricant, and the total testing period was 9 h. To enable measurements running effectively also on the uncoated samples, several adaptions and compromises had to be made: in addition to reducing the applied load during the long-term tests to 0.4 MPa, this load was not applied directly in full, but stepwise, *i.e.*, starting at 0.15 MPa and increasing the load every 3 min by 0.5 MPa until the full load was reached. If the foils stuck to each other or if the circular foil detached from the PDMS pin, the measurement was interrupted, the circular samples were cleaned and reattached to the PDMS pins, and the test was restarted (on the same area of the rectangular samples as before) but the time for each load step until the full load was reached was reduced to 90 s each. The resulting CoF was recorded twice per minute; additionally, to evaluate the measurement reliability, the following three parameters were traced:

- 'sets': average number of sets required to identify a set of samples effectively enabling a tribological measurement (if the measurement initiation was unsuccessful for ~7 times, a new sample set was used)
- 'runs': average number of effective measuring runs required per set of samples to achieve the full run time
- '(re-)starts': average number of measurement initiations required per set of samples to achieve the full run time

Once the full runtime of 9 h (running at full load) was reached on a set of samples, the measurement was terminated.

2.8. Confocal laser scanning microscopy

Confocal laser scanning microscopy was conducted using a VK-X1000 microscope (Keyence, Oberhausen, Germany) equipped with a 20x magnification lens (CF Plan, NA = 0.46; Nikon, Chiyoda, Tokyo, Japan). Prior to performing the measurements, all samples were dried and cleaned with particle-free pressurized air. Then, the samples were placed onto a glass slide using a droplet of distilled water as a thin spacer to allow the measuring device to automatically differentiate between the

very thin, transparent foils and the glass slide.

For samples that had been exposed to the long term tribological testing, the entire visible contact area was captured as one stitched image. Therefore, the lubricant employed for the long-term tests was removed by thoroughly cleaning the samples in ddH_2O.

To derive quantitative surface roughness parameters from the captured images, the software MultiFileAnalyzer (Keyence) was used. To preprocess the images, first, a linear tilt was removed; second, the sample waviness (a wave form with correction strength of 10 out of 20) was subtracted; third, artefact valleys (created when the measurement process penetrated into the transparent material) were removed by inverting the height, cropping the peaks (employing medium intensity as defined by the program), and inverting the height once more such that the sample was in its original orientation again. On each adjusted topographical image, a rectangular area ($\sim 7\ mm^2$) was defined that was located centrally within each contact area. Then, the following metrological parameters (based on ISO 25178-2) were calculated: the root-mean-square-height S_q:

$$S_q = \sqrt{\frac{1}{A}\int\int_A z^2(x,y)\ dx\ dy} \tag{1}$$

and the peak extreme height S_{xp} which is defined as the difference in height z between an areal material ratio of 2.5% and of 50%. This set of parameters was chosen as S_q is a frequently used surface roughness parameter giving a general overview over the height distribution of a sample surface. Additionally, S_{xp} was selected as a peak-related parameter to detect any signs of wear or abrasion generated in response to the long-term treatment.

2.9. Resilience assessments

Coated samples were exposed to different application-oriented treatments to compare the resilience of the coatings towards such relevant processes. Subsequently, those coated and treated samples were examined by employing linear tribology tests, surface zeta potential measurements, a surface morphology analysis, and FTIR scans (see SI 4 & 5).

2.9.1. UV disinfection

For treatment with ultraviolet light, samples were immersed into PBS, placed into a commercial UV sterilization chamber (BLX-254; Vilber-Lourmat GmbH, Eberhardzell, Germany) and exposed to UV light (wavelength of 254 nm; 4 × 8 W) for 1 h.

2.9.2. Storage

To assess the storability of the samples, coated samples were UV disinfected and dipped into 80% ethanol (to avoid bacterial contamination) and then stored either immersed in PBS at $T = 7\ °C$ (cold) or at $T = 30\ °C$ (warm) or dehydrated and stored at T~ 21 °C (dry).

2.9.3. Sterilization

Two different sterilization methods were applied. Treatments with γ-irradiation ('gamma'; dose: 25–50 kGy; system type: JS9000; complied standards: EN ISO 9001, EN ISO 13 485, EN ISO 11137-1) or ethylene oxide ('ETO'; duration: 5 h, temperature: 45 °C, pressure: 610 mbar, average ETO concentration: 700 mg L^{-1}) were conducted by employing commercial standard processes available at the company steripac GmbH (Calw, Germany). For both treatments, the samples were stored in sterilization bags.

2.9.4. Evaluation measurements after resilience treatments

2.9.4.1. Linear tribology measurements. Coated samples subjected to either of the treatments described above were examined employing linear tribology to investigate the influence of the different treatments on the coating functionality, *i.e.*, the tribological performance of the coated foils. If the samples were previously stored or treated in a dried state, they were rehydrated in PBS at 7 °C for at least 24 h. The average contact pressure was set to 0.5 MPa, data points were acquired every 20 s, and the maximal run time was 20 min. In case the foils stuck to each other during testing, the measurement was terminated preliminarily. Then, this shortened run time, *i.e.*, the time for which the movable foil slid over the fixated foil without the autohesive foils sticking together, was defined as effective run time and traced for all samples in addition to the CoFs.

2.9.4.2. Surface zeta potentials. Zeta potentials for bare, coated, as well as coated and treated foil surfaces were determined using a SurPASS 3 Eco device (Anton Paar) equipped with an adjustable gap measuring cell for planar samples (Cat. No. 159880, Anton Paar). To avoid (re-)hydration effects of the coatings or substrates affecting the measurements in different ways, all samples were stored in PBS for at least 4 h prior to any measurement. A set of two identical samples was inserted into the measuring cell and the gap height was adjusted to a value between 95 µm and 110 µm. Prior to each measurement, the cell was flushed at least twice with an electrolyte solution (2% PBS at pH 7.4).

2.9.4.3. Fourier-transformed infrared spectroscopy. The FTIR spectra were acquired using a Nicolet iS50 Smart ITX ATR Diamond - FTIR spectrometer. Spectra were recorded at a 2 µm resolution, with 20 scans per sample, and in acquisition mode attenuated total reflectance (ATR). Spectra were detected for wavenumbers ranging from 4000 cm^{-1} to 525 cm^{-1} and evaluated in absorbance format. The background was characterized by scanning the empty sample stage only.

3. Results and discussion

To identify the most suitable lubricant to be combined with the two examined coatings, the friction responses obtained with different lubricants are compared. On uncoated samples, all four macromolecular lubricants show a similar and clearly improved lubricity compared to ddH_2O (Fig. 1a). Only at very high sliding velocities above ~ 200 mm/s this trend is reversed. However, those high sliding speeds are not relevant for biomedical applications, where velocities over a few hundred mm/s are rarely exceeded [40–42].

If lubricated with ddH_2O only, samples carrying either a carbo-coating (Fig. 1b) or a dopa-coating (Fig. 1c) return similar coefficients of friction (CoF) as uncoated samples. However, once combined with one of the macromolecular lubricants, a strong decrease of the CoF is observed, especially in the boundary and mixed lubrication regime, resulting in CoFs constantly below 0.04 (which is not achieved when using either coatings or lubricants only).

Next, a linear tribology setup is employed, which enables measuring the friction response between two identical samples, *i.e.*, two polymeric foils carrying the same coating. Here, a reciprocating motion is applied at a constant frequency and stroke length. The CoFs determined for either coating/lubricant combination (Fig. 1d-e) are around ~ 0.1 or below and stable over time. Owing to the strongly autohesive behavior of the PCU films (glass transition temperature $T_g = -10°C$ [46], transition range confirmed by DSC scans, see SI 2) used here and in all following tests [11], it is not possible to reliably measure samples carrying either only a coating (and not a biopolymer lubricant) or samples carrying no coating. Consistent with the results of the rotational tribology measurements, CM-Dex solutions somewhat outperform the other lubricant options for both coating variants; consequently, all further measurements are conducted with this lubricant.

Prior to assessing the durability of the coatings, their thickness is analyzed. Therefore, images depicting the sideview of the samples are captured *via* scanning electron microscopy; here, the bulk material and the interface (containing the surface coatings) are clearly differentiable (Fig. 2). Consequently, the thickness of the coatings can be estimated by

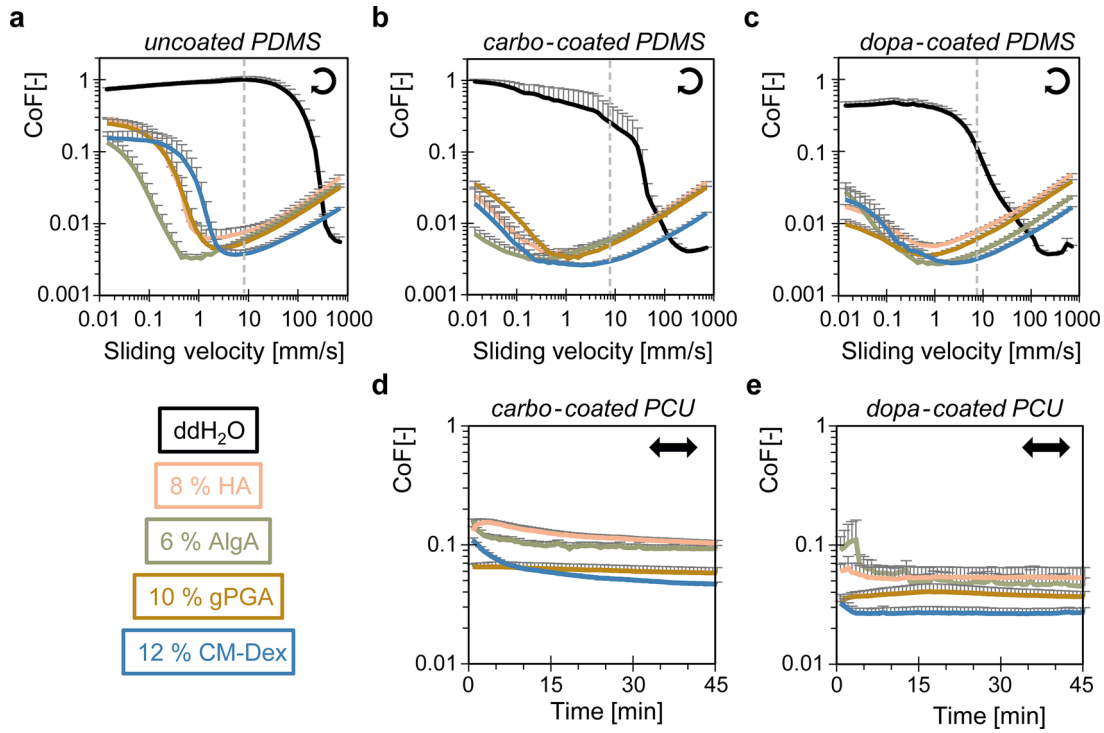

Fig. 1. *Lubrication performance of bio-macromolecular solutions on differently coated polymer substrates:* **a)** – **c)** static contact (rotational tribology setup; steel on PDMS) and **d)** & **e)** migrating contact (using two identically coated PCU films) results for a) uncoated, b) & d) carbo-coated, or c) & e) dopa-coated samples. The legend (referring to the used lubricant) applies to all subfigures. Error bars depict the standard error of the mean as determined from at least three sets of samples.

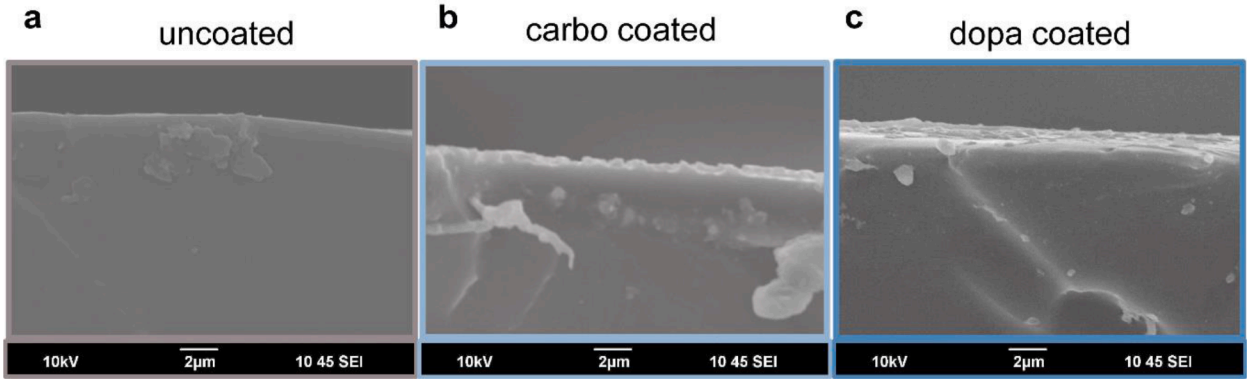

Fig. 2. *SEM images of (un-)coated PCU films:* representative SEM images acquired from side-views of a) uncoated, b) carbo-coated, and c) dopa-coated PCU-foils are displayed.

subtracting the mean interface thickness determined for uncoated samples from the mean interface thickness determined for both coated samples and applying error propagations. With this approach, a thickness d for the carbo-coating and the dopa-coating of $d_{carbo} \approx (0.25 \pm 0.07)$µm and $d_{dopa} \approx (0.95 \pm 0.29)$µm), respectively, is estimated. The individual values determined for the interface thicknesses can be found in SI 3.

To assess the durability of the very thin coatings, first extended linear tribology measurements (total run-time: 9 h) are performed and the influence of the coatings on wear generation is assessed. For comparison, measurements on uncoated samples are conducted as well. Such long-term tests are possible for all samples (Fig. 3a-c). However, they require varying effort as indicated by the number of sample sets needed to effectively start a measurement (if the measurement initiation was unsuccessful for ~7 times, a new sample set was used). For carbo-coated samples, each set allows for starting a measurement; for uncoated samples, typically two sets are required. During the measurement, the carbo-coated samples show a highly reproducible behavior without any stick-slip-effects and without any interruption of the sliding movement. Uncoated and dopa-coated samples return less steady CoF traces; moreover, for both sample types, several interruptions of the sliding movement occur, and several measurement initiations/restarts are required. This undesirable behavior is also associated with wear generation: for uncoated samples, scratches and surface distortions are clearly visible after tribological treatment; in contrast, carbo-coated samples show now clear signs of wear (Fig. 3d-e).

On tribologically treated dopamine-coated samples, some surface distortions are observed (Fig. 3f). For surface morphologies of single images of the different coating/treatment combinations, see SI 4. Surface roughness parameters derived from such profilometric images confirm this impression: the root mean square height S_q and the peak extreme height S_{xp} remain constant for carbo-coated samples; in contrast, for the other two samples, those two parameters are increased by the tribological treatment (Fig. 3g–h). Thus, it can be concluded that the carbo-coating provides better wear protection.

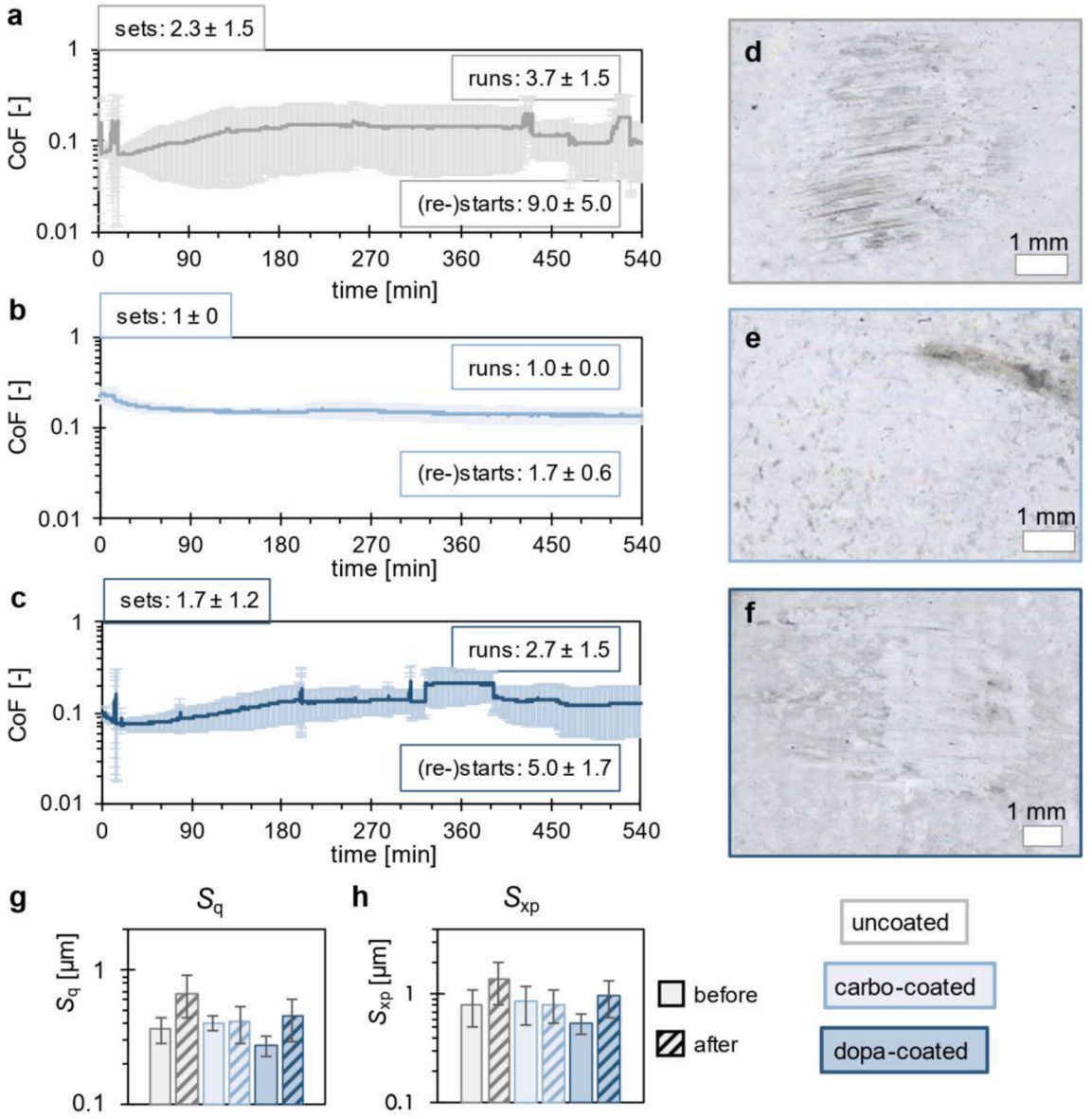

Fig. 3. *Long-term tribological treatment of the coatings:* **a) - c)** average CoF determined during linear tribology measurements running for 9 h. For definitions of 'sets', 'runs', and '(re-)starts', see method section (2.7). **d) – f)** exemplary profilometric images of (coated) samples after treatment. **g) – h)** comparison of two surface roughness parameters before and after treatment. The legend below f) applies to all subfigures, the legend next to h) applies to g) and h). Error bars depict the standard deviation as determined for at least 3 (sets of) samples.

Next, the resilience of the coatings towards different storing conditions (Fig. 4) and sterilization methods (Fig. 5) is compared. In addition to the CoF, the effective runtime (eRT; maximum runtime per measurement: 20 min) is monitored, which is defined as the time for which the movable foil slides over the fixated foil without the autohesive foils sticking together. A coating/lubricant combination is rated to be functional if it continuously separates the two foils. In those tests, always the same lubricant is used; thus, differences in the tribological performance of the systems are dictated by the coating.

To avoid bacterial contaminations, all samples used for storage tests were disinfected by treating them with UV-irradiation; accordingly, UV-treated coated samples serve as an additional reference group (Fig. 4a). Such UV treatment has only an effect on the surface charge of the carbo-coated samples (*bottom diagram*), which is probably caused by interactions of the UV irradiation with the silane layer [47] used during the carbo-coating process. The tribological behavior of the carbo-coatings seems not to be affected by the UV treatment; however, the CoFs recorded for dopa-coatings are slightly increased (*top diagram, bars*). Nonetheless, both UV-treated coatings enable successful lubrication as they achieve decent CoFs of ~ 0.1 and eRTs of 20 min (*top diagram, circles*).

For samples stored at different conditions, the obtained CoFs are plotted over the eRTs (Fig. 4b-d). In such a diagram, a well-performing coating would lie in the bottom right area of the diagram; and indeed, this is where most of the carbo-coatings are located independent of their storage conditions. In contrast, dopa-coatings tend to show increased

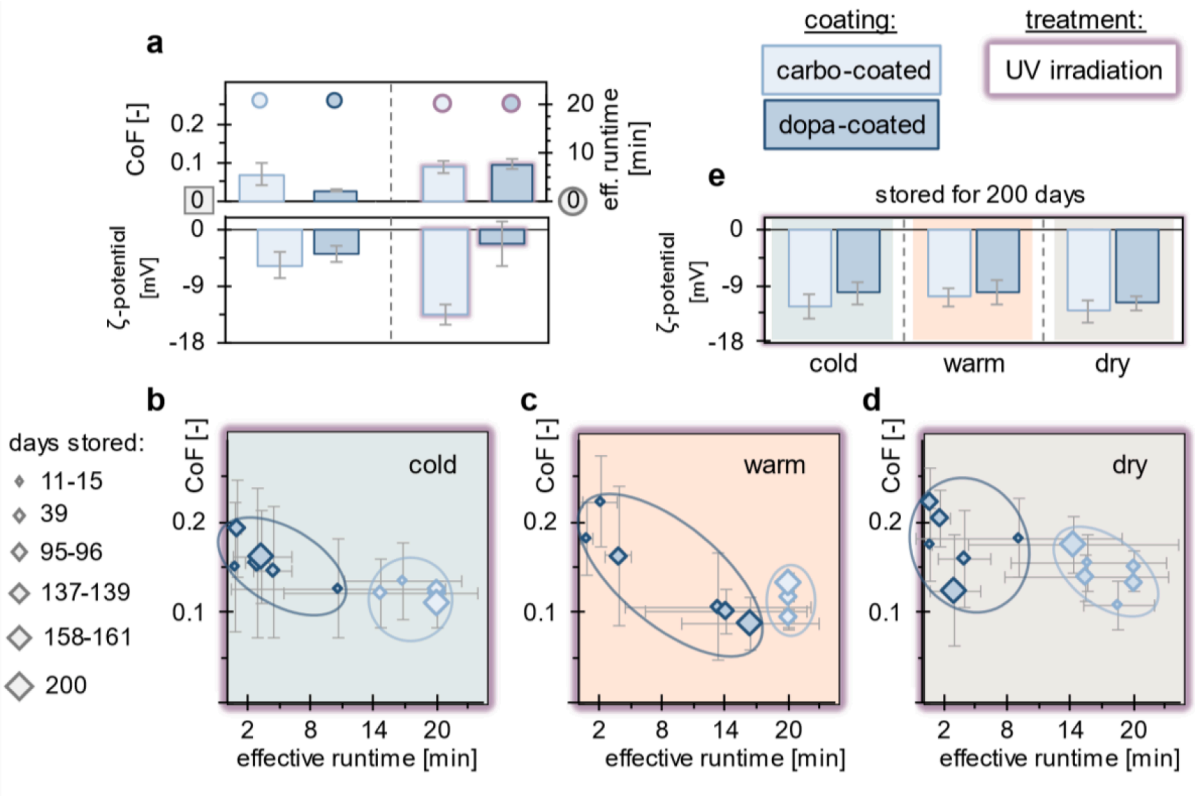

Fig. 4. *Influence of storage conditions on the coatings:* In **a),** in addition to untreated samples (left), coated and UV-treated samples (right) are shown as references. For **b)-d)** the samples were either stored b) cold, c) warm, or d) dry. e) Surface zeta potentials (at pH = 7.4) of coated samples stored for 200 days. The legend above e) applies to all subfigures, the legend next to b) applies to b) - d). For all tribology measurements, 12% CM-Dex was used as a lubricant. Error bars depict the standard error of the mean as determined from at least three sets of samples.

CoFs and/or reduced eRTs. Possibly, the dextrans bound to the dopamine layer detach over time, thus exposing the sticky dopamine layer; this, in turn, would trigger a rapid inhibition of the relative movement between the foils. However, an unexpected behavior is observed for both coatings when stored 'warm': here, the carbo-coating enables successful lubrication for each tested sample even after a storage period of 200 days with only weakly increased CoFs. Furthermore, the lubrication performance of the dopa-coated samples, which suffers after short periods of storage, appears to improve again with longer storage times. Such a behavior might be explainable by consecutive failure of the two layers comprising the coating, *i.e.,* if first the dextran layer detaches and later also the sticky dopamine-layer detaches from the PCU foils. Independent of the storage condition, the surface zeta potentials of carbo-coated samples remain unchanged when compared to the UV-treated references samples (Fig. 4b-d). In contrast, dopa-coated samples exhibit decreased surface potentials, which underscores the previous notion that those coatings are not fully stable over time.

However, for many medical devices, disinfection is not sufficient, but sterilization is required. Thus, next, the influence of common sterilization methods, *i.e.,* treatments with ethylene oxide or with γ-irradiation, on the coatings are examined. Since such sterilization processes can also affect the bulk material [48], alterations in the behavior of uncoated samples are monitored as well (Fig. 5, *white symbols*). Moreover, since the full sterilization processes (which include sample drying, shipment forth and back, sterilization, degassing, and rehydration) are very time-consuming, the sterilized samples are compared to stored samples (which were prepared and tested on the same days).

In line with our expectation, the storing process itself has hardly any influence on the friction response of the uncoated and carbo-coated samples; however, the response of the dopa-coated samples is somewhat affected. Interestingly, the uncoated material appears to be affected by the sterilization processes as the eRT is reduced to less than 2 min for ethylene oxide treated samples and to less than 1 min for γ-irradiated samples. In contrast, both coatings seem to mitigate this undesired effect. A similar picture emerges when analyzing the surface zeta potentials (Fig. 5, *bottom*): Storage of the uncoated material leads to a strong decrease of the overall surface charge, but this effect is reduced by the coatings. The same trend is obtained for the sterilized samples and confirmed by FTIR scans (as well as images of the surface morphologies, see SI 4), for which the most strongly influenced wavenumber ranges, which are associated with aliphatic hydrogen vibrations, are depicted in Fig. 5c. Here, both coatings appear to offer improved resistance to the sterilization treatments, with carbo-coated samples experiencing basically no change and the dopa-coated samples only minor changes compared to the uncoated samples (for the full FTIR scans as well as a detailed analysis and discussion of the observed bands, see SI 5). Overall, for all presented evaluations, the carbo-coated samples appear to be affected the least.

4. Conclusions

With both coating types, two PCU surfaces can be sufficiently lubricated to allow for a smooth relative sliding movement. During long-term load or storage, the more labor-intensive carbodiimide-mediated

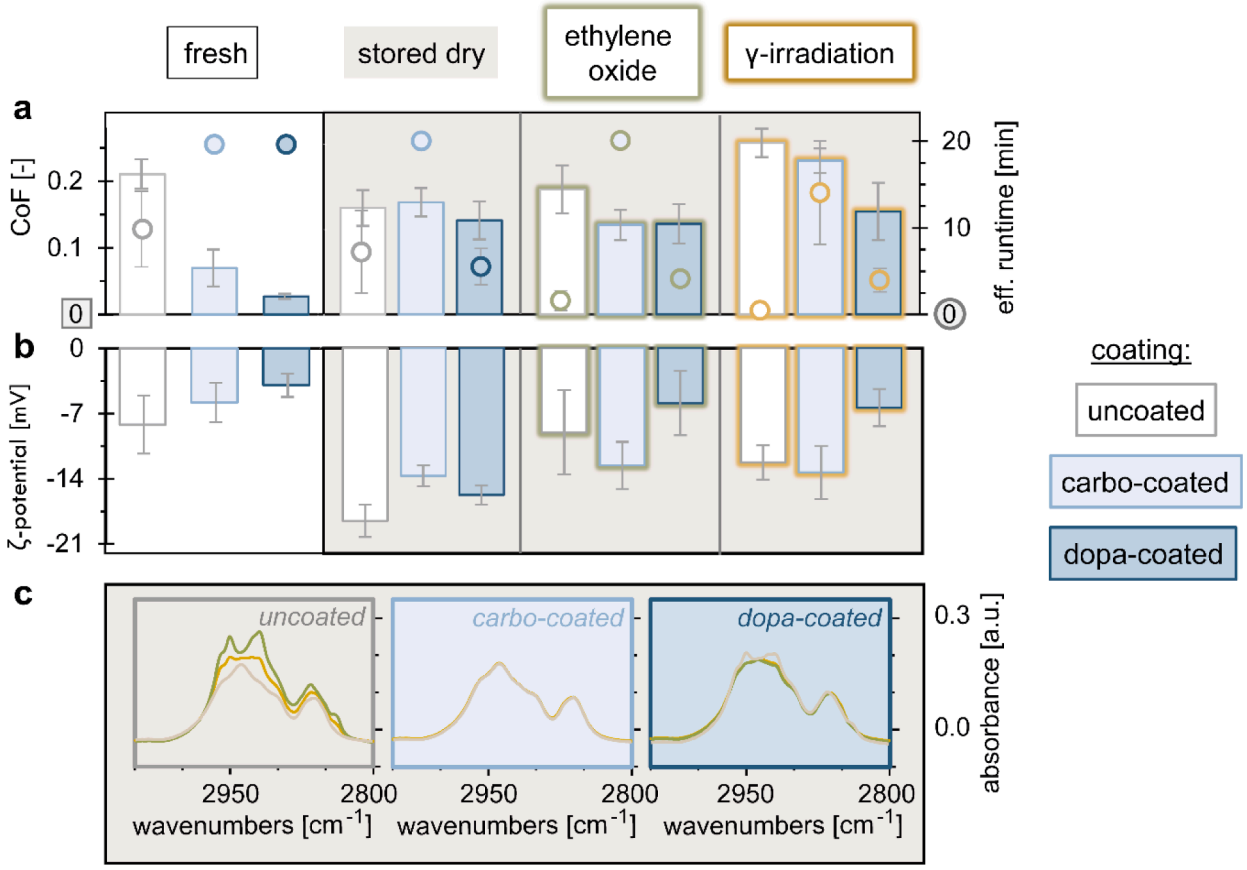

Fig. 5. *Influence of sterilization processes on the coatings:* a) linear tribology results (lubricated with 12% CM-Dex), b) surface zeta potential measurements (at pH = 7.4), and c) FTIR scans for uncoated (white/gray), carbo-coated (light blue), or dopa-coated (dark blue) samples after treatment with ethylene oxide (green outline/curve) or with γ-irradiation (yellow outline/curve). References: freshly prepared samples (white background) and stored (but unsterilized) samples (beige background). Error bars depict the standard error of the mean as determined from at least three sets of samples.

coatings outperform the easy-to-generate dopamine-coatings; this holds true with regard to reliability, the ability to avoid stick-slip events, and durability.

Statement of ethics approval

Approval of ethics is not required for the experiments conducted in this manuscript.

CRediT authorship contribution statement

Conceptualization and writing of the original draft: M.G.B. and O.L.; Data curation, formal analysis, investigation, methodology, and visualization: M.G.B., except for all content regarding DSC measurements: K. B., investigation of FTIR scans: K.B., and data acquisition and formal analysis of SEM images: L.R.; Funding acquisition, resources, supervision: O.L., J.T.; Writing (reviewing and editing): all authors;

Declaration of Competing Interest

The authors declare that they have no known competing financial interests or personal relationships that could have appeared to influence the work reported in this paper.

Data availability

The data that support the findings of this study are available from the corresponding author upon reasonable request.

Acknowledgments

The authors thank their APRICOT project partners at the Fraunhofer Institute for Manufacturing Engineering and Automation (IPA, Stuttgart, Germany) for procuring and supplying the extruded Carbothane™ films. This project has received funding from the European Union's Horizon 2020 research and innovation program under grant agreement No 863183. This publication represents the views of the author(s) only. The European Commission is not responsible for any use that may be made of the information it contains.

Supplementary materials

Supplementary material associated with this article can be found, in the online version, at doi:10.1016/j.surfin.2023.103231.

References

[1] J. Joseph, R.M. Patel, A. Wenham, J.R. Smith, Biomedical applications of polyurethane materials and coatings, Trans. IMF 96 (2018) 121–129, https://doi.org/10.1080/00202967.2018.1450209.
[2] R. Yoda, Elastomers for biomedical applications, J. Biomater. Sci. Polym. Ed. 9 (1998) 561–626, https://doi.org/10.1163/156856298X00046.
[3] S. Kumar, D.N. Roy, V. Dey, A comprehensive review on techniques to create the anti-microbial surface of biomaterials to intervene in biofouling, Colloid Interface Sci. Commun. 43 (2021), 100464, https://doi.org/10.1016/j.colcom.2021.100464.
[4] H.Y. Ahmadabadi, K. Yu, J.N. Kizhakkedathu, Surface modification approaches for prevention of implant associated infections, Colloids Surf. B 193 (2020), 111116, https://doi.org/10.1016/j.colsurfb.2020.111116.

[5] A.B. Asha, Y. Chen, R. Narain, Bioinspired dopamine and zwitterionic polymers for non-fouling surface engineering, Chem. Soc. Rev. 50 (2021) 11668–11683, https://doi.org/10.1039/d1cs00658d.

[6] N.J. Irwin, M.G. Bryant, C.P. McCoy, J.L. Trotter, J. Turner, Multifunctional, low friction, antimicrobial approach for biomaterial surface enhancement, ACS Appl. Bio Mater. 3 (2020) 1385–1393, https://doi.org/10.1021/acsabm.9b01042.

[7] J. Song, B. Winkeljann, O. Lieleg, Biopolymer-based coatings: promising strategies to improve the biocompatibility and functionality of materials used in biomedical engineering, Adv. Mater. Interfaces 7 (2020), 2000850, https://doi.org/10.1002/admi.202000850.

[8] J.L. Lanigan, S. Fatima, T.V. Charpentier, A. Neville, D. Dowson, M. Bryant, Lubricious ionic polymer brush functionalised silicone elastomer surfaces, Biotribology 16 (2018) 1–9, https://doi.org/10.1016/j.biotri.2018.08.001.

[9] F. Poncin-Epaillard, G. Legeay, Surface engineering of biomaterials with plasma techniques, J. Biomater. Sci. Polym. Ed. 14 (2003) 1005–1028, https://doi.org/10.1163/156856203769231538.

[10] H. Rashidi, J. Yang, K.M. Shakesheff, Surface engineering of synthetic polymer materials for tissue engineering and regenerative medicine applications, Biomater. Sci. 2 (2014) 1318–1331, https://doi.org/10.1039/c3bm60330j.

[11] M.G. Bauer, O. Lieleg, Bio-macromolecular surface coatings for autohesive, transparent, elastomeric foils, Macro Materials & Eng (2023) 2200681. doi:10.1002/mame.202200681.

[12] H. Lee, S.M. Dellatore, W.M. Miller, P.B. Messersmith, Mussel-inspired surface chemistry for multifunctional coatings, Science 318 (2007) 426–430, https://doi.org/10.1126/science.1147241.

[13] S. Hong, Y.S. Na, S. Choi, I.T. Song, W.Y. Kim, H. Lee, Non-covalent self-assembly and covalent polymerization co-contribute to polydopamine formation, Adv. Funct. Mater. 22 (2012) 4711–4717, https://doi.org/10.1002/adfm.201201156.

[14] J. Jiang, L. Zhu, L. Zhu, B. Zhu, Y. Xu, Surface characteristics of a self-polymerized dopamine coating deposited on hydrophobic polymer films, Langmuir 27 (2011) 14180–14187, https://doi.org/10.1021/la202877k.

[15] J.H. Ryu, P.B. Messersmith, H. Lee, Polydopamine surface chemistry: a decade of discovery, ACS Appl. Mater. Inter. 10 (2018) 7523–7540, https://doi.org/10.1021/acsami.7b19865.

[16] J. Song, T.M. Lutz, N. Lang, O. Lieleg, Bioinspired dopamine/mucin coatings provide lubricity, wear protection, and cell-repellent properties for medical applications, Adv. Healthc. Mater. 10 (2021), e2000831, https://doi.org/10.1002/adhm.202000831.

[17] Y.H. Ding, M. Floren, W. Tan, Mussel-inspired polydopamine for bio-surface functionalization, Biosurf. Biotribol. 2 (2016) 121–136, https://doi.org/10.1016/j.bsbt.2016.11.001.

[18] F. Liu, X. Liu, F. Chen, Q. Fu, Mussel-inspired chemistry: a promising strategy for natural polysaccharides in biomedical applications, Prog. Polym. Sci. 123 (2021), 101472, https://doi.org/10.1016/j.progpolymsci.2021.101472.

[19] M.E. Lynge, P. Schattling, B. Städler, Recent developments in poly(dopamine)-based coatings for biomedical applications, Nanomedicine 10 (2015) 2725–2742, https://doi.org/10.2217/nnm.15.89.

[20] C. van Mai, Di Li, H. Duan, Phenolic-compound-based functional coatings: versatile surface chemistry and biomedical applications, Langmuir 39 (2023) 1709–1718, https://doi.org/10.1021/acs.langmuir.2c03227.

[21] B. Winkeljann, M.G. Bauer, M. Marczynski, T. Rauh, S.A. Sieber, O. Lieleg, Covalent mucin coatings form stable anti-biofouling layers on a broad range of medical polymer materials, Adv. Mater. Interfaces 7 (2020), 1902069, https://doi.org/10.1002/admi.201902069.

[22] H.G. Khorana, The chemistry of carbodiimides, Chem. Rev. 53 (1953) 145–166, https://doi.org/10.1021/cr60165a001.

[23] J.V. Staros, R.W. Wright, D.M. Swingle, Enhancement by N-hydroxysulfosuccinimide of water-soluble carbodiimide-mediated coupling reactions, Anal. Biochem. 156 (1986) 220–222, https://doi.org/10.1016/0003-2697(86)90176-4.

[24] G.T. Hermanson, Bioconjugate Techniques, 3rd ed., Elsevier/AP, London, Waltham MA, 2013.

[25] B.R. Coad, M. Jasieniak, S.S. Griesser, H.J. Griesser, Controlled covalent surface immobilisation of proteins and peptides using plasma methods, Surf. Coat. Technol. 233 (2013) 169–177, https://doi.org/10.1016/j.surfcoat.2013.05.019.

[26] J. Klein, Hydration lubrication, Friction 1 (2013) 1–23, https://doi.org/10.1007/s40544-013-0001-7.

[27] D. Laage, T. Elsaesser, J.T. Hynes, Water dynamics in the hydration shells of biomolecules, Chem. Rev. 117 (2017) 10694–10725, https://doi.org/10.1021/acs.chemrev.6b00765.

[28] M. Marczynski, K. Jiang, M. Blakeley, V. Srivastava, F. Vilaplana, T. Crouzier, O. Lieleg, Structural alterations of mucins are associated with losses in functionality, Biomacromolecules 22 (2021) 1600–1613, https://doi.org/10.1021/acs.biomac.1c00073.

[29] B.T. Käsdorf, F. Weber, G. Petrou, V. Srivastava, T. Crouzier, O. Lieleg, Mucin-inspired lubrication on hydrophobic surfaces, Biomacromolecules 18 (2017) 2454–2462, https://doi.org/10.1021/acs.biomac.7b00605.

[30] B. Winkeljann, P.-M.A. Leipold, O. Lieleg, Macromolecular coatings enhance the tribological performance of polymer-based lubricants, Adv. Mater. Interfaces (2019), 1900366, https://doi.org/10.1002/admi.201900366.

[31] J. Kim, M.K. Chaudhury, M.J. Owen, Hydrophobic recovery of polydimethylsiloxane elastomer exposed to partial electrical discharge, J. Colloid Interface Sci. 226 (2000) 231–236, https://doi.org/10.1006/jcis.2000.6817.

[32] D.T. Eddington, J.P. Puccinelli, D.J. Beebe, Thermal aging and reduced hydrophobic recovery of polydimethylsiloxane, Sens. Actuators B 114 (2006) 170–172, https://doi.org/10.1016/j.snb.2005.04.037.

[33] J. Klein, Polymers in living systems: from biological lubrication to tissue engineering and biomedical devices, Polym. Adv. Technol. 23 (2012) 729–735, https://doi.org/10.1002/pat.3038.

[34] Q. Hu, Y. Lu, Y. Luo, Recent advances in dextran-based drug delivery systems: from fabrication strategies to applications, Carbohydr. Polym. 264 (2021), 117999, https://doi.org/10.1016/j.carbpol.2021.117999.

[35] S. Tiwari, R. Patil, P. Bahadur, Polysaccharide based scaffolds for soft tissue engineering applications, Polymers (2018) 11, https://doi.org/10.3390/polym11010001.

[36] M.H. Gil (Ed.), Carbohydrates Applications in Medicine, Research Signpost, Trivandrum, Kerala, India, 2014.

[37] W.B. NEELY, Dextran: structure and synthesis, Adb. Carbohyd. Chem. 15 (1960) 341–369, https://doi.org/10.1016/S0096-5332(08)60191-5.

[38] K. Imamura, A. Fukushima, K. Sakaura, T. Sugita, T. Sakiyama, K. Nakanishi, Water sorption and glass transition behaviors of freeze-dried sucrose-dextran mixtures, J. Pharm. Sci. 91 (2002) 2175–2181, https://doi.org/10.1002/jps.10218.

[39] K. Boettcher, S. Grumbein, U. Winkler, J. Nachtsheim, O. Lieleg, Adapting a commercial shear rheometer for applications in cartilage research, Rev. Sci. Instrum. 85 (2014) 93903, https://doi.org/10.1063/1.4894820.

[40] K.-A. Kwon, R.J. Shipley, M. Edirisinghe, D.G. Ezra, G. Rose, S.M. Best, R. E. Cameron, High-speed camera characterization of voluntary eye blinking kinematics, J. R. Soc. Interface 10 (2013), 20130227, https://doi.org/10.1098/rsif.2013.0227.

[41] M. Klarhöfer, B. Csapo, C. Balassy, J.C. Szeles, E. Moser, High-resolution blood flow velocity measurements in the human finger, Magn. Reson. Med. 45 (2001) 716–719, https://doi.org/10.1002/mrm.1096.

[42] M. Grimmer, A.A. Elshamanhory, P. Beckerle, Human lower limb joint biomechanics in daily life activities: a literature based requirement analysis for anthropomorphic robot design, Front. Robot. AI 7 (2020) 13, https://doi.org/10.3389/frobt.2020.00013.

[43] H. Hertz, Ueber die Berührung fester elastischer Körper, CRLL 1882 (1882) 156–171, https://doi.org/10.1515/crll.1882.92.156.

[44] I.D. Johnston, D.K. McCluskey, C.K.L. Tan, M.C. Tracey, Mechanical characterization of bulk Sylgard 184 for microfluidics and microengineering, J. Micromech. Microeng. 24 (2014) 35017, https://doi.org/10.1088/0960-1317/24/3/035017.

[45] B. Winkeljann, A.B. Bussmann, M.G. Bauer, O. Lieleg, Oscillatory tribology performed with a commercial shear rheometer, Biotribology 14 (2018) 11–18, https://doi.org/10.1016/j.biotri.2018.04.002.

[46] The Lubrizol Corporation, Aromatic Carbothane™ AC Series TPU: Transparent Thermoplastic Polyurethane, 2020. https://www.lubrizol.com/Health/Medical/Polymers/Carbothane-TPU (Accessed 12 July 2023).

[47] T. Iline-Vul, N. Kanovsky, D. Yom-Tov, M. Nadav-Tsubery, S. Margel, Design of silane-based UV-absorbing thin coatings on polyethylene films, Colloids Surf. A 648 (2022), 129164, https://doi.org/10.1016/j.colsurfa.2022.129164.

[48] E.-S.A. Hegazy, T. Sasuga, M. Nishii, T. Seguchi, Irradiation effects on aromatic polymers: 1. Gas evolution by gamma irradiation, Polymer 33 (1992) 2897–2903, https://doi.org/10.1016/0032-3861(92)90074-7.